

Contents lists available at [SciVerse ScienceDirect](#)

Journal of Controlled Release

journal homepage: www.elsevier.com/locate/jconrel

Two-layered injectable self-assembling peptide scaffold hydrogels for long-term sustained release of human antibodies

Sotirios Koutsopoulos*, Shuguang Zhang

Center for Biomedical Engineering, Massachusetts Institute of Technology, 77 Massachusetts Avenue, Cambridge, MA 02139, USA

ARTICLE INFO

Article history:

Received 10 January 2012

Accepted 15 March 2012

Available online xxxxx

Keywords:

Drug delivery
Controlled release
Multi-layer hydrogel
Protein diffusion
Self-assembly
Permeable hydrogel

ABSTRACT

The release kinetics for human immunoglobulin (IgG) through the permeable structure of nanofiber scaffold hydrogels consisting of the ac-(RADA)₄-CONH₂ and ac-(KLDL)₃-CONH₂ self-assembling peptides were studied during a period of 3 months. Self assembling peptides are a class of stimuli-responsive materials which undergo sol-gel transition in the presence of an electrolyte solution such as biological fluids and salts. IgG diffusivities decreased with increasing hydrogel nanofiber density providing a means to control the release kinetics. Two-layered hydrogel structures were created consisting of concentric spheres of ac-(RADA)₄-CONH₂ core and ac-(KLDL)₃-CONH₂ shell and the antibody diffusion profile was determined through the 'onion-like' architecture. Secondary and tertiary structure analyses as well as biological assays using single molecule analyses and quartz crystal microbalance of the released IgG showed that encapsulation and release did not affect the conformation of the antibody and the biological activity even after 3 months inside the hydrogel. The functionality of polyclonal human IgG to the phosphocholine antigen was determined and showed that IgG encapsulation and release did not affect the antibody binding efficacy to the antigen. Our experimental protocol allows for 100% IgG loading efficiency inside the hydrogel while the maximum amount of antibody loading depends solely on the solubility of the antibody in water because the peptide hydrogel consists of water up to 99.5%. Our results show that this fully biocompatible and injectable peptide hydrogel system may be used for controlled release applications as a carrier for therapeutic antibodies.

© 2012 Elsevier B.V. All rights reserved.

1. Introduction

The use of hydrogels as drug delivery carriers has been explored since the beginning of the controlled release era in the 1960s primarily focusing on synthetic polymer and animal-derived hydrogels. The first generation of hydrogels consisting of synthetic polymers did not represent an ideal system for biomedical applications due to: (i) component and degradation product toxicity (e.g., many polymers require the use of toxic cross-linkers, like glutaraldehyde, and other chemicals that pose a life threat whereas others such as polyglycolic–polylactic acid and its analogues during degradation release acids locally), (ii) post-gelation polymer swelling often causes pain in the host, and (iii) release of the active compound over brief periods of time due to the large pores of the polymer network. Furthermore, some animal-extracted biopolymers such as collagen and laminin [1,2] are not suitable for drug delivery applications in humans due to their origin and the risk of inflammatory host response from viruses, bacteria, and other unknown

substances that may be present in the donor tissue. In response to the need of biocompatible polymer drug release systems, biodegradable polymer hydrogels were developed [3–5] whereas recent advancements in the purification of hydrogel material components such as hyaluronic acid and polysaccharides open new paths for applications in humans [6,7].

Previously, a nanofiber hydrogel consisting of the self-assembling peptide ac-(RADA)₄-CONH₂ (where R is arginine, A is alanine and D is aspartic acid) was studied for controlled release of small, model-drug molecules [8]. In a recent study, it was shown that proteins with different molecular weights and isoelectric points were slowly released through the ac-(RADA)₄-CONH₂ peptide hydrogel and the release kinetics were studied over a period of 3 days [9]. Self assembling peptides form a hydrogel inside the body upon interaction of the peptide water solution with biological fluids and therefore represent an injectable drug delivery system. Upon being introduced to electrolyte solutions, self-assembling peptides form nanofibers with diameters between 10 nm and 20 nm which are further organized to form a hydrogel containing water up to ~99.5% w/v and form pores with diameter 5–200 nm [9]. Peptide gelation does not require harmful materials, such as toxic cross-linkers, to initiate the sol-gel transition while the degradation products of the hydrogel are natural amino acids, which can be metabolized and reused by the body. The fact that the sol-gel transition occurs at physiological conditions facilitates mixing of the

Abbreviations: CD, circular dichroism; IgG, immunoglobulin; PC, phosphorylcholine; FCS, fluorescence correlation spectroscopy; QCM, quartz crystal microbalance.

* Corresponding author at: Massachusetts Institute of Technology, 77 Massachusetts Av., Center for Biomedical Engineering NE47-307, Cambridge, MA 02139, USA. Tel.: +1 617 324 7612; fax: +1 617 258 5239.

E-mail address: sotiris@mit.edu (S. Koutsopoulos).

0168-3659/\$ – see front matter © 2012 Elsevier B.V. All rights reserved.
doi:10.1016/j.jconrel.2012.03.014

Please cite this article as: S. Koutsopoulos, S. Zhang, Two-layered injectable self-assembling peptide scaffold hydrogels for long-term sustained release of human antibodies, *J. Control. Release* (2012), doi:10.1016/j.jconrel.2012.03.014

peptide solution with bioactive molecules and co-injection in a tissue-specific manner to form the drug delivery vehicle in the tissue. Peptide hydrogels are biocompatible, amenable to molecular design, and have been used in a number of tissue engineering applications including bone and cartilage reconstruction, neuronal and heart tissue regeneration, wound healing, angiogenesis, and hemostasis [10–12]. Self-assembling peptide hydrogels provide a platform that makes them ideal for a wide range of bionanomedical applications as they facilitate cell migration inside the hydrogel. Furthermore they are non-toxic, non-immunogenic, non-thrombogenic, biodegradable, and applicable to localized therapies through injection into a particular tissue [12].

Long-term administration of therapeutic antibodies may be beneficial for the treatment of many diseases such as cancer, where tumor cell-specific antibodies can be used to prevent cancer relapse or metastasis after radiotherapy, chemotherapy or surgery, rheumatoid arthritis, or viral diseases in individuals with compromised immune system [13]. Currently, long term treatment with therapeutic antibodies requires frequent injections due to the limited life time of immunoglobulins in the human body (i.e., half-life is between 2 and 23 days depending on the isotype), or intravenous injection which however, carries a risk of infection, vein rupture and extravasation, hypothermia, and patient discomfort. Due to the cost associated with the production of monoclonal antibodies, alternative approaches are required in which doses might be reduced and the bioavailability is enhanced. Local and sustained antibody release reduces the number of injections and lowers the administered dose thus minimizing the adverse toxic effects associated with administration of high doses of biologically active agents. Previously, the sustained delivery of functional antibodies has been investigated using 3–8 mm solid poly(ethylene-co-vinyl acetate) polymer matrices, which however had to be implanted or immobilized in contact with the mucus vaginal environment [14], implanted polyurethane hydrogel which released the IgG load within a few hours [15], implanted carboxymethylcellulose gel which also released the load in 6–9 h [16], and more recently using an implantable pH-responsive poly(methacrylic acid) (PMAA) hydrogel [17].

We report here the sustained release of human immunoglobulin (pI 7.1, MW 146 kDa) through injectable ac-(RADA)₄-CONH₂ and ac-(KLDL)₃-CONH₂ self assembling peptide hydrogels (Fig. 1) over a period of 3 months and the release kinetics of IgG through the hydrogels. The self assembling peptide system will gel upon injection intramuscularly, subcutaneously, in the void space of the brain, in the knee joint, or in any other tissue and release therein the therapeutic antibody. This peptide hydrogel system allows for 100% loading efficiency of IgG inside hydrogels whereas due to the consistency of the hydrogel (i.e., contains water up to 99.5%) the maximum amount of antibody loading depends solely on the solubility of the antibody in water. To examine if the processes involved in incorporating and releasing the antibody from the peptide hydrogels affect its conformation and function, the released antibody was analyzed using circular dichroism (CD), fluorescent

spectroscopy and immunoassays to verify its biological activity. The functionality of IgG was monitored using single molecule fluorescence correlation spectroscopy (FCS) and quartz crystal microbalance (QCM) biosensor techniques. The presentation of functional antibodies with therapeutic properties is important for sustained delivery biomedical applications.

2. Materials and methods

2.1. Chemicals and reagents

The ac-(RADA)₄-CONH₂ and ac-(KLDL)₃-CONH₂ peptides were obtained in powder form from CPC Scientific (Sunnyvale, CA, USA) and were characterized at the MIT Biopolymers Lab (Cambridge, MA, USA). Human polyclonal IgG was purchased from Sigma-Aldrich (St. Louis, MO, USA). The pI of human IgG was 7.1 as determined by isoelectric focusing gel electrophoresis in a PhastSystem, using IPEG strips and protein standards (Bio-Rad Laboratories, Hercules, CA) and the IPGphor system (Amersham Pharmacia Biotech, Uppsala, Sweden).

2.2. IgG release experiments

Peptide hydrogels were formed using well-established protocols [8–11]. Briefly, the ac-(RADA)₄-CONH₂ and ac-(KLDL)₃-CONH₂ peptides were dissolved in deionized water and ultrasonicated using a probe sonicator for 30 min prior to use. The peptide solution in water was mixed with phosphate buffered saline (PBS, pH = 7.4) containing IgG at a final concentration of 5 μM. 40 μl of the solution mixture (i.e., peptide in PBS containing IgG) was transferred into 200-μl polypropylene tubes and gelation occurred in less than 10 min. Subsequently, 70 μl of PBS was slowly added to the 40 μl of the hydrogel which contained 5 μM IgG. To satisfy the perfect-sink conditions and allow for the determination of the protein release profile, at each time point 40 μl of the supernatant was replaced with the same volume of fresh PBS. During the course of the measurements the hydrogel volume did not change and therefore, the IgG release could not be due to hydrogel degradation or swelling. Control experiments did not show detectable adsorption of IgG on the surface of the polypropylene tubes.

Formation of a two-layer hydrogel architecture involved a two-step gelation process. The solution mixture containing 1.0% w/v ac-(RADA)₄-CONH₂ peptide and 5 μM IgG in PBS was introduced in a syringe and pushed through the needle to form a drop hanging at the tip of the needle. Then we waited 10 min to allow for gelation. The self-assembly process resulted in a hydrogel with spherical geometry. Then, using a different syringe containing a solution mixture of freshly prepared 0.6% w/v ac-(KLDL)₃-CONH₂ peptide in PBS we carefully allowed the drop of the ac-(KLDL)₃-CONH₂ solution to come in contact and encapsulate the preformed ac-(RADA)₄-CONH₂ peptide hydrogel thus creating an 'onion-like' two-layered hydrogel structure (Fig. 2). The

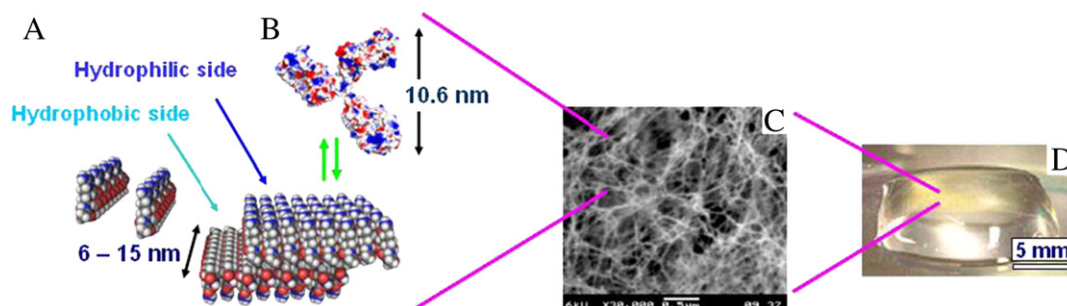


Fig. 1. Graphical representation of (A) the ac-(RADA)₄-CONH₂ peptide monomer, and of the peptide nanofiber, (B) the IgG molecule, (C) electron microscopy image of the peptide nanofibers, and (D) macroscopic image of the hydrogel. Color scheme for IgG and peptides: positively charged (blue), negatively charged (red), and hydrophobic (grey). (For interpretation of the references to color in this figure legend, the reader is referred to the web version of the article.)

two-layered hydrogel was placed in the bottom of a polypropylene tube and diffusion experiments were performed as described in the previous paragraph (Fig. 2A).

Prior to visualization of the two-layered hydrogel (Fig. 2B–D) we mixed the ac-(KLDL)₃-CONH₂ and the ac-(RADA)₄-CONH₂ peptide solutions with Alexa-488 (green) and CY3 (red) fluorescent dyes solutions, respectively. The two-layered hydrogel consists of two concentric spheres with composition 1.0% w/v ac-(RADA)₄-CONH₂ (core) and 0.6% w/v ac-(KLDL)₃-CONH₂ (shell). Visualization was performed with a fluorescence microscope (Nikon TE300, Hamamatsu camera, and Openlab image acquisition software).

The IgG release experiments through the self-assembling peptide hydrogel were performed at room temperature. The concentration of the released IgG in the supernatant was determined spectrophotometrically at 280 nm (NanoDrop ND-1000 UV-vis, NanoDrop Technologies, Delaware, USA) using a calibration curve of the native IgG at different concentrations. All data points represent the average of 4 samples. Uncertainties in the calculated parameters were estimated via common error propagation techniques, i.e., for a function $y = g(x_1, x_2)$ errors in the calculated values were determined using the equation $\sigma_y^2 = (\partial g/\partial x_1)^2 \sigma_{x_1}^2 + (\partial g/\partial x_2)^2 \sigma_{x_2}^2$.

2.3. Diffusivity determination from released IgG concentration

For a hydrogel matrix that contains a molecularly dispersed diffusing agent, the apparent diffusion coefficient may be calculated using the 1-D unsteady-state form of Fick's second law of diffusion, which for small values of time (t) is given by [6,23,24]:

$$\frac{M_t}{M_\infty} = \left(\frac{16 D_{app} t}{\pi H^2} \right)^{0.5} \quad (1)$$

where D_{app} is the apparent diffusivity, M_t and M_∞ are the cumulative mass of the diffusing compound released from the hydrogel after t and infinite time (∞), respectively. The thickness of the hydrogel matrix (H) inside the well was calculated from the volume of the peptide-IgG solution (i.e., 40 μ l) and from the dimensions of the wells of the polypropylene tubes. D_{app} may be obtained from the slope of the straight line fitting the data of M_t/M_∞ vs. $t^{0.5}$, for $0 < M_t/M_\infty < 0.6$.

2.4. Circular dichroism (CD)

Far-UV CD spectra were recorded between 190 and 260 nm at room temperature (Aviv 62DS spectrometer). CD spectra of hydrogel released IgG after 2-months were compared with those of freshly prepared IgG solutions at the same concentration. Spectra were recorded in 1-nm steps and averaged over 2 s. All measurements were carried out in 1-mm quartz cuvettes in PBS, pH 7.4. Spectra resulted from accumulation and averaging of 4 scans. Blank spectra of the buffer without IgG, obtained under identical conditions, were subtracted.

2.5. Fluorescence emission spectroscopy

Fluorescence emission of 0.3 μ M released and native IgG was measured using a Perkin-Elmer LS-50B spectrophotometer at room temperature using quartz cuvettes of 1-cm path length. Emission spectra were recorded between 310 and 400 nm on excitation at 300 nm. The excitation and emission slit widths were set at 5.0 and 2.5 nm, respectively. Sample conditions were identical to those described for the CD measurements.

2.6. FCS functionality assay of IgG

FCS characterization of the antibody-antigen binding was performed at room temperature using the Fluoropoint single molecule detection system (Olympus, Tokyo, Japan). The inherent, fluorescence signal of

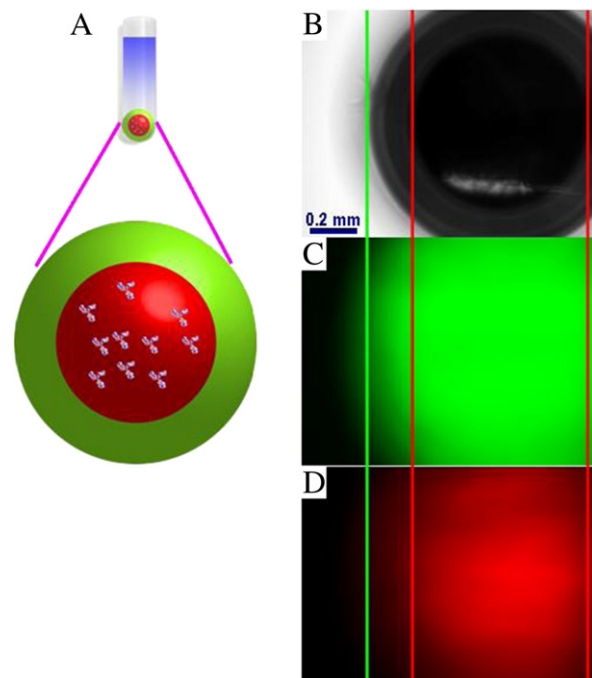


Fig. 2. (A) Schematic representation of the two-layer hydrogel system. (B) Optical and (C–D) fluorescence microscopic examinations of the two-layered hydrogels. For visualization purposes the shell (self-assembled ac-(KLDL)₃-CONH₂ peptide) contains Alexa-488 fluorophore (C) and the core (self-assembled ac-(RADA)₄-CONH₂ peptide) contains CY3 (D).

proteins due to tryptophan fluorescence is small for detection by the single molecule analysis system that we used. Therefore, we labeled human IgG with the strong fluorophore Alexa-647 using a standard protein labeling kit (Molecular Probes Inc., Eugene, OR) following the manufacturer's instructions. Briefly, the labeling protocol is based on the Alexa-647 succinimidyl ester moiety that reacts efficiently with primary amines of IgG to form stable dye-IgG conjugates. Using this protocol, IgG is labeled with an average of 4.6 Alexa-647 molecules per IgG molecule. Alexa-647 fluorescently labeled IgG molecules crossing the confocal femtoliter volume were excited by a He-Ne laser at 633 nm, measured (counts per unit time) and converted to concentration using a calibration curve of the Alexa-647 fluorescently labeled IgG at different concentrations. Fluctuations in fluorescent intensity within a confocal volume are recorded as a function of time and the autocorrelation function, $g(\tau)$, is influenced by the properties of the fluorescing molecules as well as the diffusion dynamics in the local environment [18,19]. To define the autocorrelation function for the case of anomalous 3-D diffusion of monodisperse particles in solution [18,20,21], the Fluoropoint system employed Eq. (2):

$$g(\tau) = 1 + \left(\frac{1 - F_{trip} + F_{trip} e^{-\tau/\tau_{trip}}}{N} \right) \left(\frac{1}{1 + (\tau/\tau_D)} \right) \left(\frac{1}{1 + (1/s^2) (\tau/\tau_D)} \right)^{0.5} \quad (2)$$

where $g(\tau)$ is a function of the fractional population (F_{trip}) and decay time (τ_{trip}) of the triplet state, N is the number of Alexa-647 labeled IgG molecules within the sample volume, τ_D is the translational diffusion time, and s is a factor describing the cylindrically shaped detection volume and is equal to the ratio of the radius of the cylinder's basal plane (ω_0) divided by one half of its height (ω_1). In a fully anisotropic solution, with diffusing molecules significantly smaller than the confocal volume, the diffusion coefficient D of the IgG molecules is equal to $D = \omega_0^2/4\tau_D$. The autocorrelation profile was fitted using single and multiple translational diffusion times. All data points represent the average of 4 or 8 samples.

Alexa-647 labeled IgG in PBS was allowed to interact for 1 h at room temperature with 10-fold excess PC-BSA antigen (Athera Biotechnologies AB, Sweden). Binding of IgG to the antigen would result in increased molecular weight (and size) complexes, which would be characterized by slower translational diffusion times (τ_D) compared to free IgG. The effect of non-specific binding of IgG to the antigen was evaluated by measuring the binding affinity in the presence of different concentrations of Tween detergent. At 0.05% Tween non-specific

binding was minimal and therefore, all IgG–antigen binding studies were performed at this Tween concentration. The data were analyzed using FCS algorithms as described above and the autocorrelation functions were fitted using one and multiple components.

2.7. QCM functionality assay of IgG

Biological activity of native and hydrogel released human IgG was also assessed by QCM (Attana A200, Sweden). The setup consists of a thin piezoelectric quartz disk having electrodes on each side. The quartz crystal oscillates at resonant frequencies which are sensitive to the crystal mass. As material adsorbs to the surface of the crystal, the frequency changes. To compare the binding properties of native and hydrogel released IgG, the PC-BSA antigen was covalently immobilized to the QCM channels using an amine coupling kit according to the manufacturer's instructions (Attana, Sweden). Antigen immobilization involved activation of the gold surface, which covers the quartz crystal, by 1-ethyl-3-[3-dimethylaminopropyl]-carbodiimide hydrochloride and *N*-hydroxysulfosuccinimide and then injection of 5 $\mu\text{g}/\text{ml}$ antigen dissolved in 10 mM sodium acetate solution pH 4. In a final step, we injected ethanolamine blocking solution and rinsed the surface with HBS buffer pH 7.4. Preliminary experiments showed that non-specific IgG–antigen binding was minimal in 0.05% Tween detergent and therefore, all binding studies were performed at this Tween concentration. Kinetic data at room temperature were obtained by injecting 35 μL of 20 $\mu\text{g}/\text{mL}$ human IgG for 84 s, flow rate 20 $\mu\text{L}/\text{min}$ over PC-BSA immobilized on the QCM surface and measuring the mass increase of the surface due to IgG binding to PC-BSA. The kinetic data were corrected for negative controls: (i) injection of human polyclonal IgG over a surface with immobilized BSA, (ii) injection of monoclonal anti-His tag antibody over a surface with immobilized PC-BSA, and (iii) injection of monoclonal anti-rhodopsin antibody over a surface with immobilized PC-BSA. The data were analyzed (Attaché Evaluation software) using a simple 1:1 binding model for the binding reaction between antibody and antigen. From the analysis the association, k_a , and dissociation, k_d , rate constants were calculated as well as the binding affinity constants, defined as $K_D = k_d/k_a$, of the native and released IgG for the antigen. The fitting was evaluated based on the χ^2 value and the residual error which was near zero.

3. Results and discussion

3.1. Human IgG release through the peptide hydrogel

As may be seen in Fig. 3A, an initial rapid release of IgG was observed within the first hour (burst effect). This is likely due to IgG molecules that were at or near the solvent/hydrogel interface and rapidly escaped into the supernatant solution. Inspection of Fig. 3 also shows that the initial rapid release was significant in the case of the lower density with 0.5% w/v ac-(RADA)₄-CONH₂ and 0.3% w/v ac-(KLDL)₃-CONH₂ hydrogels which reached 27% and 25% release of the total IgG loading within the first 2 h. More dense nanofiber networks, as in the case of the 1.0% w/v and 1.5% w/v ac-(RADA)₄-CONH₂ as well as in the case of the 0.6% w/v ac-(KLDL)₃-CONH₂ hydrogels showed a lower IgG burst of 15%, 10% and 3%, respectively after 2 h of release. The burst effect was not observed in the case of the two-layer 1.0% w/v ac-(RADA)₄-CONH₂ (core)–0.6% w/v ac-(KLDL)₃-CONH₂ (shell) hydrogel which showed release of less than 1% after 2 h of measurements. Previous work showed that protein release through this peptide hydrogel depends on the size of the protein [9]. Small proteins are released faster whereas IgG, which is a large protein, was released slower. Therein, it was shown that IgG release was not complete after 3 days. Here we show that IgG release through peptide hydrogels did not asymptotically reach a plateau value even after 3 months. In hydrogel systems protein release rarely reaches 100%, the reason being the physical entrapment

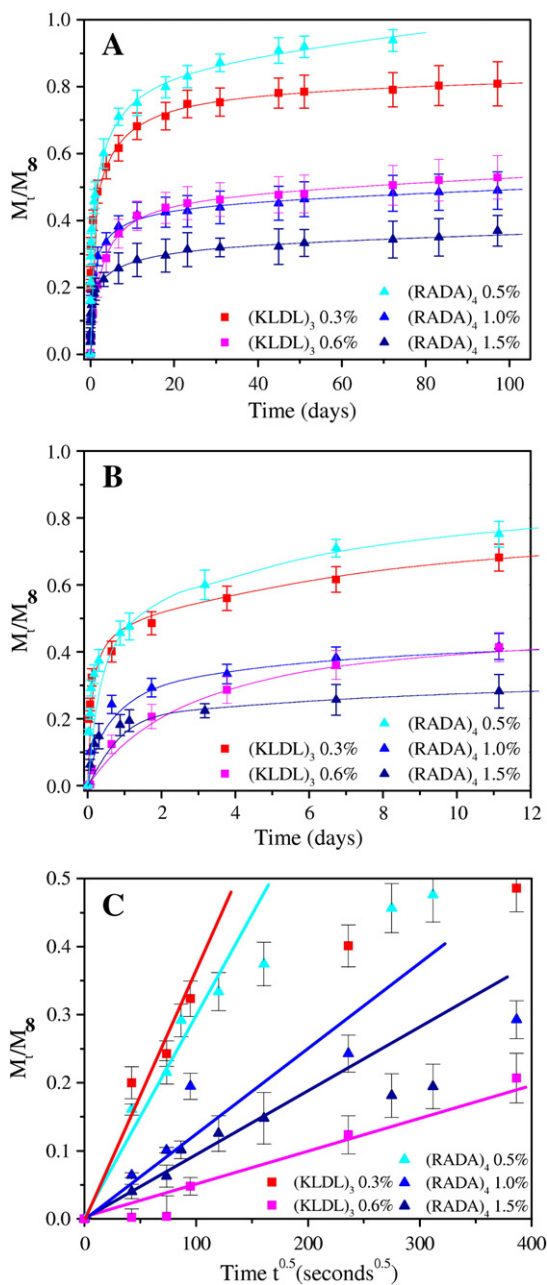


Fig. 3. The release profiles (A) during the entire 3-month period and (B) during the first 12 days for IgG through hydrogels of different peptides and different peptide nanofiber densities. Hydrogels consisted of the self assembling peptides (i) ac-(RADA)₄-CONH₂ with concentration 0.5% w/v (light blue, ▲), 1.0% w/v (blue, ▲), and 1.5% w/v (dark blue, ▲) and of (ii) ac-(KLDL)₃-CONH₂ with concentration 0.3% w/v (red, ■) and 0.6% w/v (magenta, ■). Release experiments were performed in PBS, pH 7.4 at room temperature. Data points represent the average of 5 samples. (C) IgG release plotted as a function of the square root of time showing a biphasic diffusion mechanism. The initial linear part of the plots represents simple diffusion of IgG through the peptide hydrogel and is used to calculate diffusion coefficients based on the Fick's law (Eq. (1)). (For interpretation of the references to color in this figure legend, the reader is referred to the web version of the article.)

of the protein molecules in highly entangled nanofiber domains of the hydrogel which hinder free motion of the diffusant.

3.2. The effect of peptide hydrogel density on the diffusion of human IgG

To investigate the effect of the hydrogel density on the release profiles of IgG, the self-assembling peptide concentration was varied. Increasing the peptide concentration resulted in higher density network of nanofibers which hindered the release of IgG. Fig. 3A shows

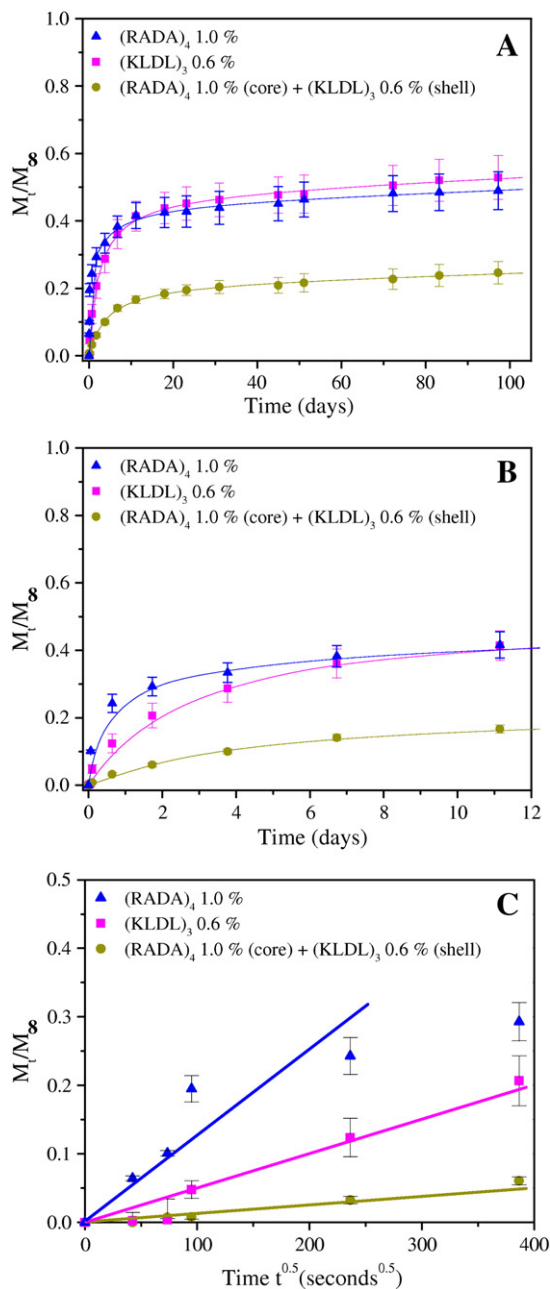


Fig. 4. The release profiles of IgG (A) during the entire 3-month period and (B) during the first 12 days, through hydrogels consisting of ac-(RADA)₄-CONH₂ with concentration 1.0% w/v (blue, ▲), ac-(KLDL)₃-CONH₂ with concentrations 0.6% w/v (magenta, ■), and two-layer, two-component hydrogel which is composed of 1.0% w/v ac-(RADA)₄-CONH₂ (core) and 0.6% w/v ac-(KLDL)₃-CONH₂ (shell) (yellow, ●). Release experiments were performed in PBS, pH 7.4 at room temperature. Data points represent the average of 5 samples. (C) IgG release is plotted as function of the square root of time showing a biphasic diffusion mechanism: the initial linear part of the plots represents simple diffusion of IgG through the peptide hydrogel and is used to calculate diffusion coefficients based on the Fick's law (Eq. (1)). (For interpretation of the references to color in this figure legend, the reader is referred to the web version of the article.)

the release kinetics of IgG through ac-(RADA)₄-CONH₂ peptide hydrogels with peptide concentrations of 0.5% w/v (99.5% water), 1.0% w/v (99% water), and 1.5% w/v (98.5% water) and though ac-(KLDL)₃-CONH₂ peptide hydrogels with concentrations of 0.3% w/v (99.7% water) and 0.6% w/v (99.4% water). Higher density ac-(KLDL)₃-CONH₂ hydrogels were not tested because such hydrogels are characterized by increased stiffness which made sample handling difficult. The results show that IgG release through the hydrogel may be controlled by varying the peptide nanofiber density.

3.3. Building complex multi-layered peptide hydrogel structures for drug release

The two-layer hydrogel system consists of two compartments. Fig. 2A and B–D shows the structure of the two-component peptide hydrogel in which each of the two components is loaded with a dye to facilitate visualization. The hydrogel sphere in the core is formed by self-assembly of the ac-(RADA)₄-CONH₂ peptide and contains the CY3 dye (red) whereas the encapsulating second sphere is composed of ac-(KLDL)₃-CONH₂ and contains the Alexa-488 (green) fluorophore. Bright-field and fluorescence microscopy show the contour of each hydrogel (Fig. 2B–D). Although diffusion of the dyes eventually results in diffusion of CY3 and Alexa-488 into the ac-(KLDL)₃-CONH₂ and the ac-(RADA)₄-CONH₂ hydrogels, respectively and homogeneous distribution throughout the entire two-component peptide hydrogel system is eventually expected, the initial distribution of the dyes clearly defines the shape and dimensions of each hydrogel sphere.

In the antibody release experiments we did not use the fluorescent dyes. Instead, the core is formed by gelation of 1.0% ac-(RADA)₄-CONH₂ peptide and is loaded with the antibody whereas the second layer (shell) consisting of the ac-(KLDL)₃-CONH₂ hydrogel does not contain antibody and it encapsulates the core. The release profile of IgG through the two-layer hydrogel system was significantly slower compared to the observed profiles in the case of simple, single component ac-(RADA)₄-CONH₂ and ac-(KLDL)₃-CONH₂ hydrogels (Figs. 3A and 4A). This may be due to differences in density and chemical properties of the nanofibers between the two hydrogels. It has been shown that the 0.6% w/v ac-(KLDL)₃-CONH₂ hydrogel forms more dense network of peptide nanofibers and appears to be stiffer even compared to the 1.5% w/v ac-(RADA)₄-CONH₂ hydrogel [10,11].

Furthermore, the formation of the two-layer hydrogel resulted in a system in which the initial protein burst release was significantly smaller compared to that observed in the one-component hydrogels. Therefore, IgG diffusion through the two-layer hydrogel results in an apparent near-zero-order diffusion profile (Fig. 4A and B). It is anticipated that a combination of additional hydrogel layers consisting of hydrogels with higher nanofiber densities would probably result in the formation of a multi-layer system with very small or no burst.

Table 1

Diffusion constants of human immunoglobulin (IgG, MW 146 kDa, $r_h = 5.3$ nm, $pI = 7.1$) in solution using the Stokes–Einstein equation and upon release through the peptide hydrogels using Fick's law. Standard deviations were calculated using error propagation ($n = 8$).

Peptide hydrogel	Hydrogel density (w/v)	Diffusion constants (10^{-10} m ² /s)	
		Stokes–Einstein estimate	Apparent in gel (Eq. (1))
ac-(RADA) ₄ -CONH ₂	0.5%	0.4	0.183 ± 0.002
	1.0%		0.028 ± 0.001
	1.5%		0.017 ± 0.001
ac-(KLDL) ₃ -CONH ₂	0.3%	0.4	0.205 ± 0.004
	0.6%		0.0040 ± 0.0001
ac-(RADA) ₄ -CONH ₂ (core) + ac-(KLDL) ₃ -CONH ₂ + 0.6% (shell)	1.0% (core) + 0.6% (shell)	0.4	0.0010 ± 0.0001

The multi-layer self assembling peptide hydrogel technology is easily transferable from bench to bedside by injecting the two peptide solutions simultaneously using for instance a two-compartment syringe with concentric needles. Gelation occurs upon interaction of the peptide solutions with biological fluids and the release of the active compound could be continuous for prolonged periods of time.

3.4. IgG diffusivity through the hydrogel scaffold

The diffusion coefficient of IgG in water at infinitely dilute conditions at 20 °C was calculated to be $0.4 \times 10^{-10} \text{ m}^2 \text{ s}^{-1}$ using the Stokes–Einstein equation $D_{S-E} = k_B T / 6\pi\eta r_h$, where k_B is the Boltzmann constant, T is the absolute temperature of the medium, η is the dynamic viscosity of the solvent (taken as 1.002 cP) and r_h is the hydrodynamic radius of IgG [22]. Using single molecule analysis of diffusing IgG molecules in PBS previously we showed that at micromolar IgG concentrations the Stokes–Einstein equation gives a good estimate of the IgG diffusivities in solution. However, inside the peptide hydrogel single molecule analysis showed that the Stokes–Einstein equation overestimates the IgG diffusivities by ~25% [9]. The Stokes–Einstein equation was developed for infinitely diluted molecules which follow Brownian motion and therefore, molecular crowding and interaction of the diffusing molecules with the peptide nanofibers of the hydrogel may affect diffusion by slowing the molecular motion.

To calculate the diffusion coefficient of IgG during release through the peptide hydrogels we used the release profiles shown in Fig. 3. Application of the commonly used Fickian model, which is described by Eq. (1), results in apparent IgG diffusion coefficients inside the hydrogel which significantly differed (i.e., between 50% and 80% depending on the type of hydrogel and hydrogel density) from those determined for IgG using the Stokes–Einstein equation (Table 1). The model of

calculating diffusion coefficients using Fick's Law was developed assuming diffusion of small molecules, infinite dilution of the diffusant, and that the diffusion of the molecules through the hydrogel solely depends on Brownian motion. In hydrogel systems these assumptions are rarely satisfied. Eq. (1) is commonly used to determine apparent diffusion coefficients even when these conditions do not apply. The reason for doing so is that it facilitates the discussion of systems when there is no other easily transferable method for determining the diffusivity. Previously, using a different experimental method, we determined apparent in-gel diffusion coefficients for IgG through the 1% w/v ac-(RADA)₄-CONH₂ hydrogel [9] which were within the same order of magnitude with the values obtained in this work.

Plotting the release data as a function of the square root of time (Fig. 3C) showed that the diffusion mechanism is biphasic. The initial linear part of each plot indicates diffusion controlled release of the IgG through the peptide hydrogel and it is used to calculate diffusion coefficients based on Fick's law [23,24]. Deviation from the straight line at longer times may be associated with non-Fickian, anomalous diffusion. Hydrogel pores with small sizes and/or diffusion hindrance due to specific interactions between diffusing IgG molecules and peptide nanofibers of the hydrogel may also account for the deviation from Fick's law.

3.5. Conformational properties of released IgG

Protein aggregation events as well as protein–peptide interactions resulting in protein inactivation could occur during IgG's residence in the peptide solution, during self-assembly and nanofiber formation, or during the release process. To obtain insight into the conformational state of hydrogel-released IgG, 2-months post encapsulation far-UV

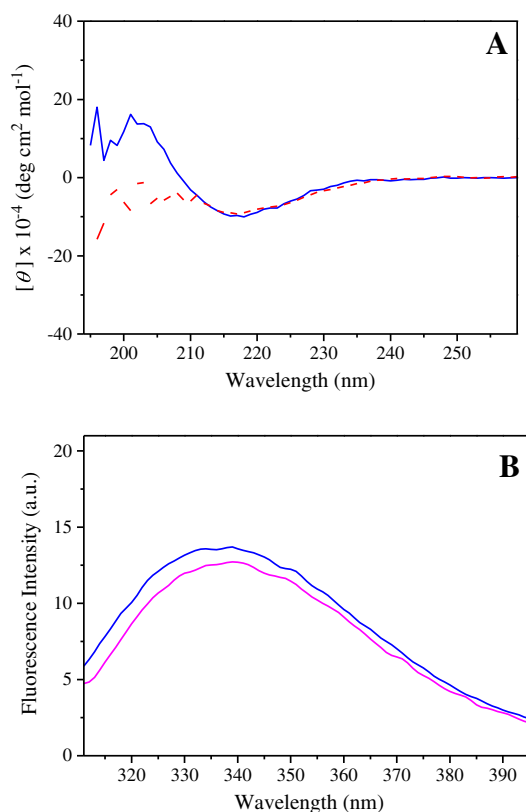


Fig. 5. Spectroscopic examination of the human IgG in PBS, pH 7.4. (A) Far-UV CD spectra of native (solid line) and peptide hydrogel released (broken line) IgG. (B) Normalized fluorescence emission spectra of the native (solid line) and released IgG (broken line) through the peptide hydrogel; excitation wavelength was 300 nm. Spectra were recorded at room temperature in 2-months post release samples.

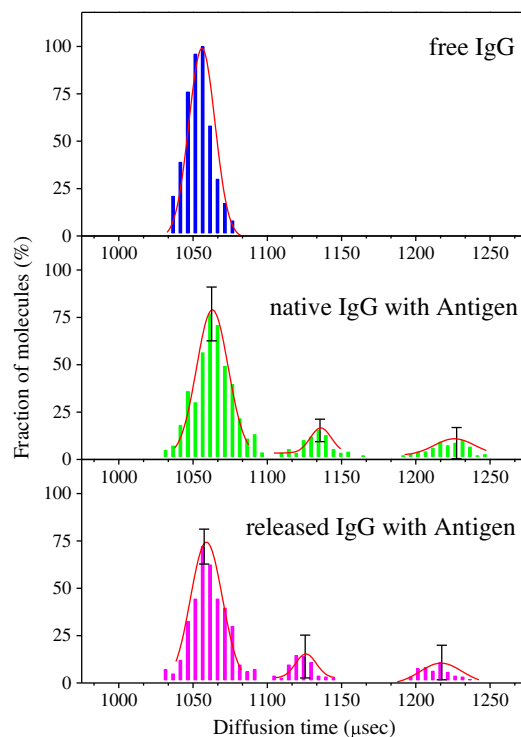


Fig. 6. Translational diffusion times of free IgG molecules in the absence and in the presence of the PC-BSA antigen before and after release through the ac-(RADA)₄-CONH₂ peptide hydrogel. FCS data showed that the interaction of IgG with the antigen resulted in three different species: free IgG molecules which had diffusion times similar to that of IgG alone, and IgG that bonds to one or two antigen molecules. The relative concentration of these species was similar before and after release of IgG. Standard deviations are between 5 and 12%.

CD and fluorescence spectroscopy were employed to examine the secondary and tertiary structural characteristics, respectively. CD spectra of native IgG were identical to those reported in the literature [25]. As may be seen in Fig. 5A, the CD spectrum of hydrogel released IgG closely resembled that of a freshly prepared IgG solution. Small deviations were observed at wavelengths below 200 nm where the diode or HT (i.e., total absorption) level was high. The relatively low concentration of released IgG, in conjunction with the possible presence of detached nanofibers from the scaffold could be reasons for the low signal-to-noise ratio observed in this region of the spectrum. However, the β -sheet content of IgG, as seen from the 218 nm ellipticity, was not affected during the release process.

Fluorescence emission spectra were recorded with excitation at 300 nm to excite the tryptophans. The emission spectrum is sensitive to the tryptophan microenvironment within the 3D structure of the protein and therefore, fluorescence emission can be used to detect tertiary structure changes of released IgG. A red shift in the wavelength of maximum emission would indicate tryptophan exposure to the polar solvent and protein unfolding. The fluorescence emission spectrum of IgG was similar with literature reports [26]. Inspection of Fig. 5B shows that at the same IgG concentration the emission spectrum of released IgG was similar to that of native IgG with respect to both the emission maximum and fluorescence intensity suggesting that IgG encapsulation and release did not induce tertiary structure changes.

3.6. Functionality assays of released human IgG

As a subpopulation of human IgGs is known to bind phosphorylcholine (PC), a common antigen which is present in many human infecting microorganisms including *Streptococcus pneumoniae* [27–30], the PC-conjugated BSA (PC-BSA) antigen was used to examine the functionality of native and hydrogel-released IgG. The PC-BSA complex that was used in this work contains approximately 17 PC molecules per BSA. The interaction of human IgG with the PC-BSA antigen was investigated using the single molecule FCS detection system. FCS data analysis was performed by fitting the autocorrelation functions using one and multiple components. The goodness-of-fit for each data set was judged by the value of the χ^2 parameter and by inspection of the residuals which were uniformly distributed around zero. In all cases the simplest model was chosen. Attempted fits of the experimental data to a model with less independent components resulted in increased χ^2 values. Control experiments of: (i) the buffer solution, (ii) unlabeled IgG molecules in the presence of the antigen, (iii) heat-denatured labeled IgG in the presence of the PC-BSA antigen, and (iv) labeled IgG in the presence of BSA (without the PC hapten) were also performed and did not reveal a measurable interaction.

Data analysis showed that one τ_D was sufficient to describe the autocorrelation function of free IgG (Fig. 6). Upon interaction of IgG with 10-fold excess PC-BSA antigen (i.e., 50 μ M), three different species were identified based on their diffusion time: the free, unbonded IgG molecules and those that bond to one or two antigen molecules (Fig. 6). Data analysis showed that free IgG molecules have a diffusion time of ca. 1060 μ s through the detection volume regardless of the presence of the antigen. A comparison of the diffusion times of IgG before and after release through the peptide hydrogel showed that the same type of IgG-(PC-BSA)_x complexes were formed upon interaction with the antigen. These complexes had diffusion times of approximately 1135 μ s and 1230 μ s corresponding to binding of IgG to one or two antigen molecules, respectively. Fig. 6 also shows that the percentage of IgG molecules in each category (i.e., free and interacting with one or two antigen molecules), before and after release through the hydrogel was similar. These results suggest that the binding affinity of IgG for the PC-BSA antigen did not change upon release from the peptide hydrogel and therefore, the biological activity of IgG is not affected by encapsulation and release through the hydrogel.

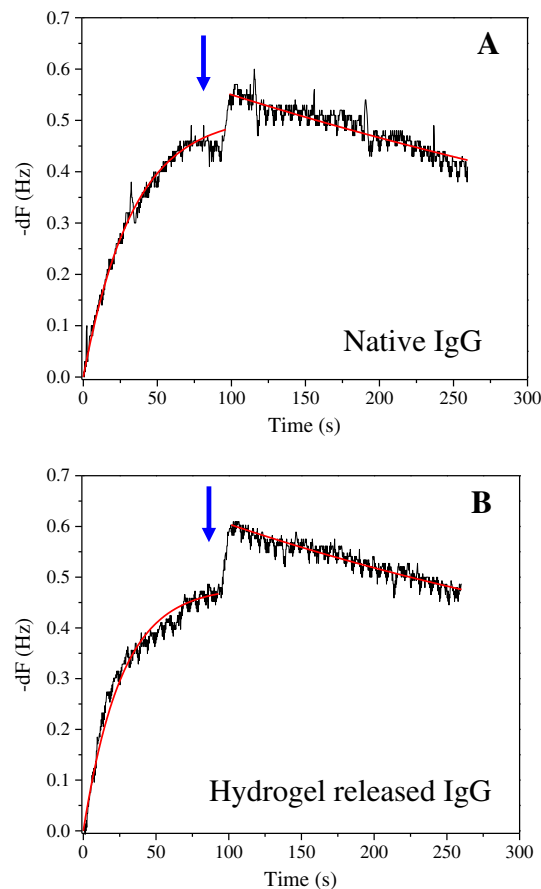


Fig. 7. QCM time-dependent frequency changes, $-dF$ (Hz), upon association (binding) and dissociation of the (A) native and (B) hydrogel released polyclonal human IgG with immobilized PC-BSA (antigen). Time zero represents injection of IgG in the flow channel which is followed by the association phase. The biosensor signal (black line) increases upon IgG binding to the immobilized antigen and decreases upon buffer injection (arrow) which results dissociation of the bound IgG. The similarity of the calculated rate constants and of the affinity constants between native and hydrogel released IgG suggests that the biological activity of IgG was not affected upon incorporation and release through the peptide hydrogel. Data fitting is represented by the red line. (For interpretation of the references to color in this figure legend, the reader is referred to the web version of the article.)

The relatively high percentage anti-PC IgG molecules (Fig. 6) in the polyclonal human IgG sample prompted further inquiry. Using a radio-immunoassay method and blood samples from several individuals, Scott et al. measured a sizable proportion of anti-PC-BSA antibodies in the human serum up to 800 μ g/ml [31]. The concentration of IgG in the human serum is ca. 8–15 mg/ml, which suggests that up to 10% of all IgGs in the human serum are specific for the PC hapten. Therefore, the relatively high percentage (i.e., ~19%) of anti-PC antibodies observed using the single molecule analysis in vitro is reasonable. In our experiments, the PC-BSA complex contains approximately 17 PC groups per BSA protein unit. This suggests that the binding observed by FluoroPoint is not due to un-specific binding but a result of high avidity of the anti-PC immunoglobulins to the PC-BSA antigen. Further work will be required to determine whether this observation can be reproduced using human IgG samples from other sources.

To test the functionality of human IgG before and after being released through the peptide hydrogel the QCM technique was also used. Criteria for IgG functionality were the kinetics of binding and the affinity constants between the monoclonal IgG and the PC-BSA antigen. Upon interaction with PC-BSA immobilized on the gold surface of the QCM, it was shown that after 2 months in the peptide hydrogel, the released human IgG did not undergo functional changes compared to the native IgG. Upon fitting of the data in Fig. 7, kinetic analysis showed that the association $k_a = 9.47 \pm 0.05 \times 10^4 \text{ M}^{-1} \text{ s}^{-1}$ and dissociation $k_d = 1.65$

$\pm 0.02 \times 10^{-3} \text{ s}^{-1}$ rate constants for the native IgG were similar to those observed for the hydrogel released IgG $k_a = 11.85 \pm 0.10 \times 10^4 \text{ M}^{-1} \text{ s}^{-1}$, $k_d = 2.39 \pm 0.02 \times 10^{-3} \text{ s}^{-1}$. Furthermore, the binding constants, $K_D = 17.4 \pm 0.2 \text{ nM}$ and $K_D = 20.2 \pm 0.2 \text{ nM}$ for the native and hydrogel released IgG, respectively were similar. These results confirm the single molecule analyses and demonstrate that the functionality of the post-release antibody was not affected by interaction with the peptide hydrogel during the course of the release experiment.

4. Conclusions

One of the main goals of sustained drug delivery is to efficiently direct therapies to specific tissues. In cases of drugs with side effects localized delivery will result in less toxicity side effects on patients. The injectable self-assembling peptide system, which gels under physiological conditions, has the potential to be a robust system for sustained release applications including immunotherapies to release active antibodies locally in specific tissues over prolonged periods of time. In this study, it is shown that human antibodies were slowly released through the ac-(RADA)₄-CONH₂ or ac-(KLDL)₃-CONH₂ peptide hydrogels for a period of over 3 months and furthermore, the release kinetics depended on the amino acid sequence of the self assembling peptides which form the hydrogel and the density of the peptide nanofibers in the hydrogel. An efficient controlled release system should present biologically active proteins. The secondary and tertiary structures of the hydrogel released antibodies as well as their biological activities were examined and we showed that they were not affected by encapsulation and release through the hydrogel. These results present an opportunity to create new tailor-made, programmable and multi-layered peptide hydrogels for sustained release of antibodies and other proteins. Peptide hydrogel systems can be easily designed and synthesized. The programmability of the peptide sequence provides a means of controlling the nanofiber properties at the molecular level which, in turn, alter the biomolecular diffusion and release kinetics. It is anticipated that further fine-tuning of the peptide hydrogel systems will allow for a wide range of applications in biomedical technology.

Acknowledgments

Dr. Hans Grönlund (Athera Biotechnologies AB, Sweden) is acknowledged for gift of the PC-BSA antigen and for useful discussions. We are thankful to Dr. Liselotte Kaiser for technical support and QCM data processing.

References

- [1] K.H. Stenzel, T. Miyata, A.L. Rubin, Collagen as a biomaterial, *Annu. Rev. Biophys. Bioeng.* 3 (1974) 231–253.
- [2] A.L. Rubin, K.H. Stenzel, T. Miyata, M.J. White, M. Dunn, Collagen as a vehicle for drug delivery, *J. Clin. Pharmacol.* 13 (1973) 309–312.
- [3] B. Jeong, Y.H. Bae, D.S. Lee, S.W. Kim, Biodegradable block copolymers as injectable drug-delivery systems, *Nature* 388 (1997) 860–862.
- [4] Y. Qiu, K. Park, Environment-sensitive hydrogels for drug delivery, *Adv. Drug Deliver. Rev.* 53 (2001) 321–339.
- [5] B.K. Davis, Control of diabetes with polyacrylamide implants containing insulin, *Experientia* 28 (1972) 348.
- [6] F.A. Kincl, L.A. Ciaccio, S.B. Henderson, Sustained release preparations, XVI. Collagen as a drug carrier, *Arch. Pharm.* 317 (1984) 657–661.
- [7] S.T. Lim, G.P. Martin, D.J. Berry, M.B. Brown, Preparation and evaluation of the in vitro drug release properties and mucoadhesion of novel microspheres of hyaluronic acid and chitosan, *J. Control. Release* 66 (2000) 281–292.
- [8] Y. Nagai, L.D. Unsworth, S. Koutsopoulos, S. Zhang, Slow release of molecules in self-assembling peptide nanofiber scaffold, *J. Control. Release* 115 (2006) 18–25.
- [9] S. Koutsopoulos, L.D. Unsworth, Y. Nagai, S. Zhang, Controlled release of functional proteins through designer self-assembling peptide nanofiber hydrogel scaffold, *Proc. Natl. Acad. Sci. U. S. A.* 106 (2009) 4623–4628.
- [10] B.C. Wang, Y.C. Wu, Z.W. Shao, S.H. Yang, B. Che, C.X. Sun, Z.L. Ma, Y.N. Zhang, Functionalized self-assembling peptide nanofiber hydrogel as a scaffold for rabbit nucleus pulposus cells, *J. Biomed. Mater. Res. A* 100 (2012) 646–653.
- [11] J. Kisiday, M. Jin, B. Kurz, H. Hung, C. Semino, S. Zhang, A.J. Grodzinsky, Self-assembling peptide hydrogel fosters chondrocyte extracellular matrix production and cell division: implications for cartilage tissue repair, *Proc. Natl. Acad. Sci. U. S. A.* 99 (2002) 9996–10001.
- [12] M.E. Davis, J.P.M. Motion, D.A. Narmoneva, T. Takahashi, D. Hakuno, R.D. Kamm, S. Zhang, R.T. Lee, Injectable self-assembling peptide nanofibers create intramyocardial microenvironments for endothelial cells, *Circulation* 111 (2005) 442–450.
- [13] S. Yoon, Y.S. Kim, H. Shim, J. Chung, Current perspectives on therapeutic antibodies, *Biotechnol. Bioprocess Eng.* 15 (2010) 709–715.
- [14] W.M. Saltzman, N.F. Sheppard, M.A. Mchugh, R.B. Dause, J.A. Pratt, A.M. Dodrill, Controlled antibody release from a matrix of poly(ethylene-co-vinyl acetate) fractionated with a supercritical fluid, *J. Appl. Polym. Sci.* 48 (1993) 1493–1500.
- [15] I.A. Rojas, J.B. Slunt, D.W. Grainger, Polyurethane coatings release bioactive antibodies to reduce bacterial adhesion, *J. Control. Release* 63 (2000) 175–189.
- [16] K.A. Poelstra, N.A. Berekzi, A.M. Rediske, A.G. Felts, J.B. Slunt, D.W. Grainger, Prophylactic treatment of gram-positive and gram-negative abdominal implant infections using locally delivered polyclonal antibodies, *J. Biomed. Mater. Res.* 60 (2002) 206–215.
- [17] L. Blasi, S. Argenti, G. Morello, I. Palama, G. Barbarella, R. Cingolani, G. Gigli, Uptake and distribution of labeled antibodies into pH-sensitive microgels, *Acta Biomater.* 6 (2010) 2148–2156.
- [18] R. Rigler, E.S. Elson, *Fluorescence Correlation Spectroscopy: Theory and Applications*, Springer, NY, 2001.
- [19] W.W. Webb, Fluorescence correlation spectroscopy: inception, biophysical experiments, and prospectus, *Appl. Opt.* 40 (2001) 3969–3983.
- [20] M.J. Saxton, Anomalous diffusion due to obstacles: a Monte Carlo study, *Biophys. J.* 66 (1994) 394–401.
- [21] O. Krichevsky, G. Bonnet, Fluorescence correlation spectroscopy: the technique and its applications, *Rep. Prog. Phys.* 65 (2002) 251–297.
- [22] J.K. Armstrong, R.B. Wenby, H.J. Meiselman, T.C. Fisher, The hydrodynamic radii of macromolecules and their effect on red blood cell aggregation, *Biophys. J.* 87 (2004) 4259–4270.
- [23] J. Crank, G.S. Park, *Diffusion in polymers*, Academic Press, NY, 1968.
- [24] T. Higuchi, Mechanism of sustained-action medication. Theoretical analysis of rate of release of solid drugs dispersed in solid matrices, *J. Pharm. Sci.* 52 (1963) 1145–1149.
- [25] K. Ikeda, K. Hamaguchi, S. Migita, Circular dichroism of Bence-Jones proteins and immunoglobulins G, *J. Biochem.* 63 (1968) 654–660.
- [26] Y. Nishiyama, Y. Mitsuda, H. Taguchi, S. Planque, M. Hara, S. Karle, C.V. Hanson, T. Uda, S. Paul, Broadly distributed nucleophilic reactivity of proteins coordinated with specific ligand binding activity, *J. Mol. Recognit.* 18 (2005) 295–306.
- [27] M.A. Leon, N.M. Young, Specificity for phosphorylcholine of six murine myeloma proteins reactive with pneumococcus C polysaccharide and B-lipoprotein, *Biochemistry* 10 (1971) 1424–1429.
- [28] L.G. Bennett, C.T. Bishop, Structure of the type XXVII *Streptococcus pneumoniae* (pneumococcal) capsular polysaccharide, *Can. J. Chem.* 55 (1977) 8–16.
- [29] C.P.J. Glaudemans, B.N. Manjula, L.G. Bennett, C.T. Bishop, Binding of phosphorylcholine-containing antigens from *Streptococcus pneumoniae* to myeloma immunoglobulins M-603 and H-8, *Immunochimistry* 14 (1977) 675–679.
- [30] D.E. Briles, J.L. Claffin, K. Schroer, C. Forman, Mouse IgG3 antibodies are highly protective against infection with *Streptococcus pneumoniae*, *Nature* 294 (1981) 88–90.
- [31] M.G. Scott, D.E. Briles, P.G. Shackelford, D.S. Smith, M.H. Nahm, Human-antibodies to phosphocholine. IgG anti-PC antibodies express restricted numbers of V-regions and C-regions, *J. Immunol.* 138 (1987) 3325–3331.